

Dust Library of Plasmonically Enhanced Infrared Spectra of Individual Respirable Particles

Antriksh Luthra^{1,2}, Aruna Ravi^{1,3}, Sirui Li¹, Steven V. Nystrom⁴, Zechariah Thompson⁴, and James V. Coe¹

Applied Spectroscopy

0(0) 1–9

© The Author(s) 2016

Reprints and permissions:

sagepub.co.uk/journalsPermissions.nav

DOI: 10.1177/0003702816653126

asp.sagepub.com



Abstract

This work characterizes collections of infrared spectra of individual dust particles of $\sim 4\ \mu\text{m}$ size that were obtained from three very different environments: our lab air, a home air filter, and the 11 September 2001 World Trade Center event. Particle collection was done either directly from the air or by placing dust powder from various samples directly on the plasmonic mesh with $5\ \mu\text{m}$ square holes as air is pumped through the mesh. This arrangement enables the recording of “scatter-free” infrared absorption spectra of individual particles of size comparable to the probing wavelengths whose vibrational signatures are otherwise dominated by scattering and dispersive line shape distortions. The spectra are sensitive to the amounts of various infrared active components and analysis using a Mie–Bruggeman model for mixed composition particles provides volume fractions of the components. Inhalation of dust particles of $\sim 4\ \mu\text{m}$ size has significant health consequences as these are among the largest inhaled into people’s lungs. The chemical composition of $\sim 4\ \mu\text{m}$ respirable particles is of great interest from health, atmospheric, and environmental perspectives as different environments may pose different hazards and spectroscopic challenges.

Keywords

Library of infrared spectra of individual dust particles, spectroscopic determinations of volume fractions of dust components, Mie–Bruggeman model of mixed composition dust particles, inhalable dust

Date received: 29 December 2015; accepted: 4 March 2016

Introduction

Dust is omnipresent—when people breathe, airborne particulates are inhaled. Increases in particulate matter are known to be correlated with increases in all-cause mortality.¹ While definitive results^{2–4} and regulations (<https://www.epa.gov/criteria-air-pollutants/naaqs-table>) exist for $\text{PM}_{2.5}$ (particulate matter less than $2.5\ \mu\text{m}$ in aerodynamic diameter), it should be noted that these designations generally correspond to measurements with filters having 50% cutoffs at the designated size⁵ (see Figure 10–45 therein), i.e., a fair fraction of $4\ \mu\text{m}$ particles get through a $\text{PM}_{2.5}$ filter. Furthermore, simulations of human alveolar mass deposition as a function of size^{5,6} (see Chapter 10 in Hinds⁷) predict a significant coarse particle deposition distribution, particularly with open mouth breathing, with a maximum near $4\ \mu\text{m}$. Airborne particulate matter in the range of $2.5\text{--}10\ \mu\text{m}$ ($\text{PM}_{2.5-10}$) includes the largest particles that get past our noses and throats, making it into our lungs.⁷ Such particles do not stay airborne as long as smaller particles,⁸ so particles of the $\sim 4\ \mu\text{m}$ target size may be more indicative of the local

environment than the smaller particles that are inhaled fully into the lungs. Given the important and challenging issues associated with coarse particles of $\sim 4\ \mu\text{m}$ size regarding health and regulations,^{2,9} note that these experiments provide a different, size-selective, analytical perspective since the plasmonic metal mesh employed in this work captures a very narrow particle size distribution ($\sim 4.0 \pm 0.3\ \mu\text{m}$). Given the known symptoms of inhaling high levels of particulate matter and the risks associated with long-term exposure to elevated

¹Department of Chemistry and Biochemistry, The Ohio State University, USA

²Department of Mechanical and Aerospace Engineering, The Ohio State University, USA

³Department of Electrical and Computer Engineering, The Ohio State University, USA

⁴Department of Chemical Engineering, The Ohio State University, USA

Corresponding author:

James V. Coe, 100 West 18th Avenue Columbus, Ohio 43210-1173 USA.
Email: coe.1@osu.edu

levels, there is a need to chemically evaluate such particles.¹⁰ Our previous single particle work^{10–15} includes the study of a spectral library of 63 individual dust particles extracted from our laboratory air¹² demonstrating chemical variability including minerals, sulfates, nitrates, and organics, as well as a model for analysis of volume fractions.¹⁰ In this work, the study is extended to samples obtained from a home air filter and the 11 September 2001 World Trade Center (WTC) event. A Mie–Bruggeman spectral model for samples of mixed particles¹⁰ has been commonly applied to samples from the three different dust environments providing volume fractions of the common components in these samples. The Mie–Bruggeman spectral model is also shown to aid in the single value decomposition analysis of the dust library.

Fourier transform infrared (FTIR) spectroscopy offers molecular characterization of chemical functional groups in individual dust particle samples,^{12,16–20} including quantitative analysis,¹⁰ which complements the more numerous studies characterizing atoms.^{2,21–25} But to quantitatively study sub-wavelength scale dust particles, infrared (IR) spectroscopy has challenges:¹⁴ (1) vibrational peaks of wavelength-sized particles are dominated by Mie scattering effects that can be ten times larger; (2) vibrational lineshapes are distorted by dispersive scattering contributions, the Christiansen effect;^{26,27} and (3) insignificant intensity of light is transmitted to the detector through apertures as the particle falls in the micrometer-scale size range, i.e., it is smaller than the probing wavelength and detector element. Synchrotron free electron lasers with IR microscopy adaptations²⁸ offer new capabilities and can overcome the latter problem (although at significantly more expense), but are still subject to scattering effects. Benchtop FTIR instruments using blackbody sources have been used to study dust grains collected from space;^{29,30} however, again there are scattering issues. In our novel approach, the aforementioned spectroscopic challenges can be avoided by taking IR spectra of particles while they are trapped in a plasmonic metal film, providing a metallic but transmitting confinement for the particle. Particles are trapped using a pump that passes air through the mesh. The mesh has interesting optical properties including the reduction of scattering effects and the production of undistorted vibrational lineshapes of a trapped individual particle.^{31,32} The Coe group has recorded IR spectra of individual subwavelength particles including live yeast cells,¹¹ latex microspheres,^{32,33} and calibrant materials¹⁰ (quartz, gypsum, carbonates, different types of clay, humic acid/salt). This work applies a common analysis¹⁰ to three dust samples, including dust from lab air,¹⁰ a home air filter,¹⁵ and the September 11, 2001 World Trade Center event by using plasmonic Ni mesh and an imaging FTIR microscope.

Experimental

The experimental setup for recording single particle spectra of wavelength scale particles has been described in

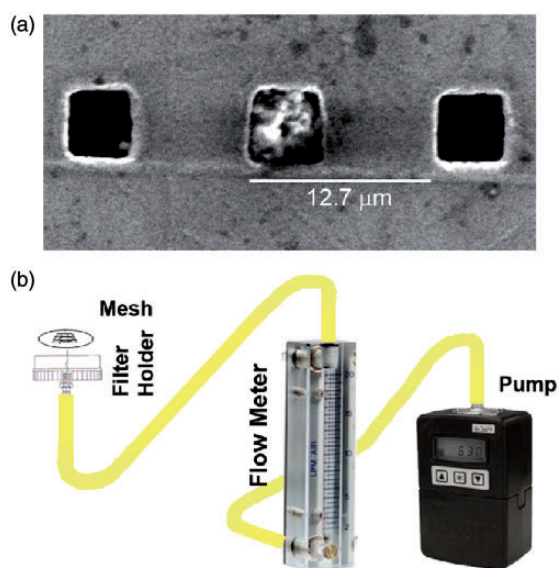


Figure 1. (a) A single dust particle trapped in a $5\ \mu\text{m}$ hole of Ni plasmonic mesh. (b) Schematic of system for pumping air through a plasmonic mesh (which replaces the filter of a typical setup). Particles can be trapped either from the air or by placing powdered samples directly on the mesh as air is pumped through the mesh.

detail elsewhere.^{10–12,15,34} The particles are trapped in a metal film with an array of microholes, plasmonic Ni mesh,^{10,12,15} having a $12.6\ \mu\text{m}$ square lattice parameter, $5\ \mu\text{m}$ square hole size, and $\sim 2\ \mu\text{m}$ thickness as available from Precision Eforming (Cortland, NY; <http://www.precisioneforming.com>). Briefly, dust sample powder is placed over the mesh and air is sucked through it using a pump that traps globular particles having widths that are slightly smaller than the mesh holes. A scanning electron microscope (SEM) image of a particle trapped in a plasmonic mesh is shown in Figure 1. The mesh is positioned under a Spotlight 300 imaging FTIR microscope (Perkin Elmer, Waltham MA) in imaging mode ($6.25\ \mu\text{m}$ by $6.25\ \mu\text{m}$ pixel size, 512 scans, $700\text{--}4000\ \text{cm}^{-1}$ range, and $4\ \text{cm}^{-1}$ resolution) using a 16 channel liquid nitrogen cooled MCT detector. A 3 pixel by 3 pixel region without a dust particle serves as a background for the same size region with a dust particle, and spectra of dust particles are only accepted if all of the surrounding holes are empty. The individual spectra have also had their baselines flattened as there is a generic rise in extinction due to the change in lensing associated with the generic increase in the index of refraction of such particles. Spectra were recorded from a total of 186 dust particles from three different environments, and 95 calibrant particles of known composition were also analyzed in this way. Calibration with particles of known composition and similar size is extremely important as it controls for any residual plasmonic or particle size effects. A description is given below for the dust library from each environment.

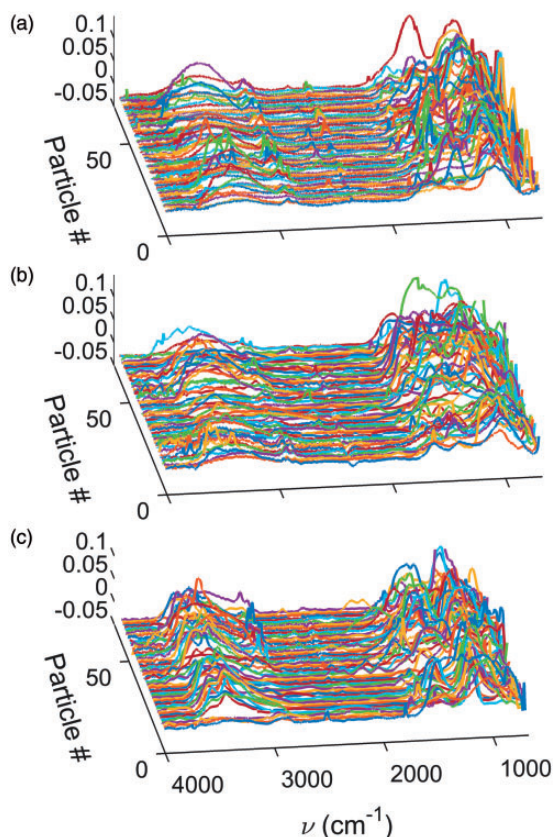


Figure 2. (a) Single particle IR spectral libraries of lab air dust; (b) dust from a household filter; (c) dust from the 11 September 2001 World Trade Center event.

Lab Air Dust

A library of IR spectra of 63 individual particles captured from our laboratory air in room 0055 of Evans Lab at the Ohio State University on 21 April 2010 was presented in our preliminary study.¹⁰ This work explored the potential of this new technique, and the plasmonically enhanced results showed that it can be used to identify not only the major components in dust, but also minority components. Figure 2a shows IR absorption spectra of the dust particles of $\sim 4\ \mu\text{m}$ size range. This work was published before a quantitative model predicting chemical composition in the average IR spectra had been developed.

Home Air Filter Dust

The less-open home environment giving rise to indoor airborne dust includes additional sources such as combustion in heating and cooking, tobacco smoke, pet dander, dried insect fragments, and human skin flakes. Household air systems such as air conditioners and central heating systems usually have furnace filters that are designed to stop dust particles from entering the heating and cooling systems, as well as people's lungs. These filters decrease the amount of

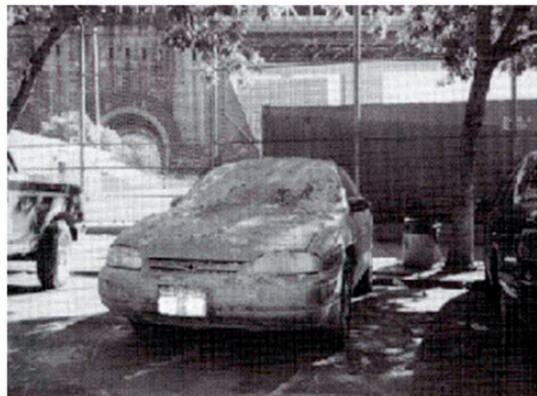


Figure 3. Dust settled on car near the intersection of Market and Water streets about 1.2 miles from “ground zero” of the 11 September 2001 World Trade Center Event. The dust was collected on 17 September 2001 and made available to us, courtesy of Dr. Paul J. Lioy. The picture is reprinted with permission from “Dust: The Inside Story of Its Role in the September 11th Aftermath”, by Paul J. Lioy, Rowman and Littlefield Publishers.

dust and bacteria circulating indoors. A pleated paper filter that collected dust over a four month period (nominally $20'' \times 25'' \times 6''$, Aprilaire 201 Research Products Corp.) in a residence was used as the source of dust for this project. Filters like this might capture $\sim 90\%$ of the particulate in the $3\text{--}10\ \mu\text{m}$ size range. The dust was collected in a plastic bag by shaking the filter, then a scoop of the dust powder was placed on the Ni mesh while pumping air through the mesh. Figure 2b shows the IR absorption spectra of 63 dust particles obtained from the home filter. In America, people spend $\sim 90\%$ of their time indoors³⁵ on average, so it is important to develop methods to characterize the respirable dust that is inhaled.

New York City 11 September 2001 World Trade Center Event

On 11 September 2001 the World Trade Center was attacked, resulting in the collapse of the Twin Tower buildings. A large plume of dust was released into the atmosphere. The plume was transported by winds to the east and southeast across New York City.³⁶ Samples of the dust were collected from various places around ground zero to assess the danger associated with exposure to the dust at different locations. The sample in this study was collected by Paul Lioy and coworkers near the intersection of Market Street and Water Street, 1.9 km away from ground zero in a weather-protected location on 17 September 2001 from the top of a car's hood as shown in Figure 3. Note that robust studies have been reported on this sample by Paul Lioy and coworkers,^{36,37} this work, however, concentrates on $\sim 4\ \mu\text{m}$ particles that might have potentially been inhaled by people near the plumes. Figure 2c shows IR absorption spectra of

60 individual dust particles from this sample. This sample is very different than the dust that individuals commonly encounter, and might be described as an example of a hazardous environment where even a single high exposure could lead to serious health consequences.

Results and Discussion

Mie Theory and Calibrant Fits

The combination of particles of comparable size to the probing wavelength and the strong vibrational spectra of common mineral components of dust^{10,14} warrant the use of Mie theory, which can handle severe lineshape distortions. Mie theory³⁸ is a complete solution to Maxwell's equations describing the absorption and scattering of light by spherical particles given the spherical particle's complex index of refraction and radius. Mie theory has been widely used in climate models to estimate the extinction spectrum of subwavelength scale particles in the atmosphere³⁹ and this work incorporates Bohren and Huffman's codes.⁴⁰ The Mie model is applied in this work to the average spectrum of a library of individual spectra, not an individual particle spectrum, since the individual particles are not spherical. In other words, one assumption of our model is that the overlapping of randomly oriented particles of different shapes when adjusted to a common center of origin, will average to a sphere, validating the use of Mie theory. Previous work¹⁰ reported the complex indices of refraction versus wavelength by fitting a Mie model to the average IR spectrum of calibrants including calcite, dolomite, gypsum, illite, montmorillonite, kaolinite, polyethylene, quartz, and yeast. These were found to be the dominant components of the lab air dust.¹² The complex index of refraction of each calibrant is the square root of the complex permittivity

$$m^*(\tilde{\nu}) = \sqrt{\epsilon(\tilde{\nu})} = \sqrt{\epsilon_0 + \sum_j \frac{A_j \tilde{\nu}_{0,j}^2}{\tilde{\nu}_{0,j}^2 - \tilde{\nu}^2 - i\Gamma_j \tilde{\nu}}} \quad (1)$$

where the index j is over the vibrations of the material, A_j is the strength of a vibrational transition, $\tilde{\nu}_{0,j}$ is the position of a transition in wavenumbers, and Γ_j is the half-width at half the maximum of the vibrational feature. Given the vibrationally mediated index of refraction parameters and a particle radius of a calibrant, Mie theory can predict the IR spectrum (extinction or absorption) of a spherically averaged calibrant particle with standard formulas.

Different dust samples are likely to have different components, so it is beneficial to add calibrants as the work proceeds. Previously, there were only two groups of organic calibrants, yeast and polyethylene. Yeast serves as an IR model for living or recently living matter, while polyethylene serves as a model for hydrocarbons that end up in rocks on

geological timescales and eventually in dust. Humic acid/salt has been added to the list of calibrants as a model for dirt-like substances, something in between living and long-dead. Humic acid was purchased commercially from Alfa Aesar, Thermo Fisher Scientific, Ward Hill MA, in the form of crystalline powder that is a mixture of the acid (50–60%) and sodium salt. The humic acid/salt is a mixed polymer assembly of aromatic and other functional groups that is intended to serve as an IR calibrant for the group of humic substances that are associated with the biodegradation of dead organic matter and are major constituents of soil, peat, coal, stream deposits, dystrophic lakes, and ocean water. Humic acid/salt is only one of a variety of such substances and serves here as a test of whether this type of calibrant is useful. Details of the Mie model for humic acid/salt are described in the supplemental information. The parameters of the other calibrants have been previously published.¹⁰ The fit is workable, but not as good as the other calibrants because the material is not a single compound.

Mie–Bruggeman Model

Typical individual dust particles have two or more components, so a model for mixtures has been developed that combines Mie theory with the Bruggeman mixture theory in order to model the average IR spectrum of mixed component dust libraries. The Bruggeman relation provides a constraint between the effective permittivity (ϵ_{eff}) of a mixture and the permittivities (ϵ_i) and volume fractions (f_i) of each component in the mixture

$$\sum_i f_i \frac{\epsilon_i - 2\epsilon_{\text{eff}}}{\epsilon_i + 2\epsilon_{\text{eff}}} = 0 \quad (2)$$

It is difficult to analytically solve for the effective dielectric (particularly with ten components), so an iterative numerical approach was used with an initial guess of

$$\epsilon_{\text{eff},k-1} = \sum_i^n f_i \epsilon_i$$

where each ϵ_i is determined by fitting the calibrant's average spectrum as discussed in the previous section and f_i were determined manually by looking at comparison plots. Rearranging Eq. 2 gives the iterative formula for the permittivity of the mixture

$$\epsilon_{\text{eff},k} = \frac{\sum_{i=0}^{n-1} \frac{f_i \epsilon_i}{\epsilon_i + 2\epsilon_{\text{eff},k-1}}}{\sum_{i=0}^{n-1} \frac{f_i}{\epsilon_i + 2\epsilon_{\text{eff},k-1}}} \quad (3)$$

Convergence is usually observed in <10 iterations. Just as for the calibrants, input of ϵ_{eff} for a certain mixture of components and a specific radius for the particle enables

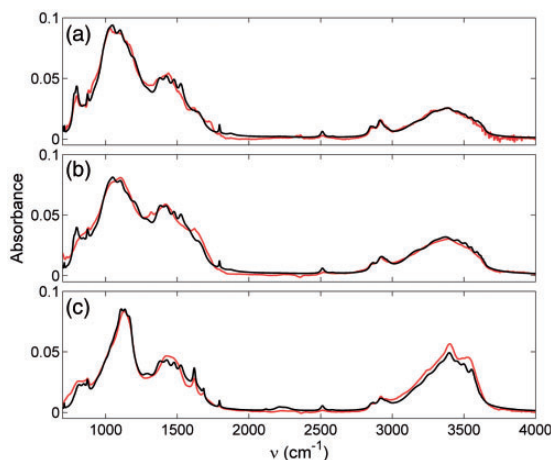


Figure 4. Mie–Bruggeman model fits of the samples from (a) lab air; (b) a house filter; (c) the 11 September 2001 World Trade Center event. The volume fractions resulting from these fits are given in Table I.

the prediction of an IR absorption spectra by standard Mie formulas. This predicted spectrum is compared to the experimental average IR spectrum for a dust library, and the volume fractions are varied until good agreement is obtained between the prediction and experiment. A Fortran program was written that performed an unweighted, nonlinear least squares fit using a parameter grid search method⁴¹ that adjusted the volume fractions and particle radius until reasonable fits were obtained as shown in Figure 4. A red trace was used for the experimental average IR spectrum for each dust library case, and a black trace was used for the Mie–Bruggeman model fit. The program was somewhat nonstandard because at each grid step of a fitted variable, the program renormalized the volume fractions so that they always added up to 1. The estimated standard deviation of the fit is computed by summing the squares of deviations between the average spectrum and the best Mie–Bruggeman fit, assuming equal weights at each wavenumber step, and dividing by the number of degrees of freedom. After the final iteration, the uncertainties of all parameters were estimated by numerically calculating the sums of the mixed second derivatives of the fit with respect to changes in the parameters. Error estimates came from the diagonal elements of the variance–covariance matrix after inverting the Hessian and scaling by the estimated standard deviation of the fit. The best fit volume fractions and their uncertainties for each case are presented in Table I.

Lab Air Dust. The Mie–Bruggeman volume fraction analysis was redone on the average IR spectrum of 63 particles by adding one more calibrant, i.e., humic acid/salt. The optimized fit of the average dust spectrum of 63 particles is shown in Figure 4a. The lab air dust with an effective radius of 1.944(25) μm was found to have volume percentages of 34% organic matter (10% yeast-like and 18% humic acid/salt-like), 25% clay (mostly illite), 4.6% gypsum, 24% quartz,

Table I. Fitted volume fractions from Mie–Bruggeman model predictions of the average IR spectra of dust from three different environments.

Calibrant	Lab air	Home filter	WTC 11 September 2001
Calcite	0.117(2)	0.102(3)	0.105(4)
Dolomite	0.003(2)	0.017(3)	0.011(3)
Gypsum	0.047(6)	0.011(7)	0.503(14)
Illite	0.243(10)	0.124(10)	0.00
Kaolinite	0.00(0)	0.00(0)	0.00
Montmorillonite	0.006(6)	0.059(10)	0.00
Polyethylene	0.056(5)	0.018(5)	0.024(7)
Quartz	0.242(6)	0.152(6)	0.017(7)
Yeast	0.102(6)	0.096(10)	0.082(12)
Humic acid/salt	0.181(10)	0.418(13)	0.255(16)

and 11% carbonates (mostly calcite). The value of the estimated standard deviation of the fit was 0.0026 in absorbance units, which is 3.3% of the maximum peak, an improvement over the previously obtained result.¹⁰

House Filter Dust. The value of the estimated standard deviation of the fit was 0.0029 in absorbance units, which is $\sim 4\%$ at the maximum peak. With an effective radius of 1.955(3) μm , it was found to have volume percentages of 52% organic matter (10% yeast-like and 42% humic acid/salt-like), 18% clay (mostly illite), 1.1% gypsum, 11.3% carbonates (mostly calcite), and 15% quartz.

World Trade Center Dust. This sample was known to have gypsum, carbonates, organics, and quartz. The value of the estimated standard deviation of the fit was 0.0033 in absorbance units, which is $\sim 4\%$ at the maximum peak. With an effective radius of 1.875(3) μm , it was found to have volume percentages of 51% gypsum, 36% organic matter (mostly 8% yeast-like and 26% humic acid/salt-like), 11% carbonates (mostly calcite), and 2% quartz. The results of this study agree with the fine particle study of McGee et al.⁴² according to which gypsum and carbonates are the major components, with quartz being the minor component. Both of these results vary from the bulk sample analysis⁴³ because the composition of dust changes dramatically with particle size⁴ (see Figure 1 therein). It is interesting to note the differences in the categories of components between a bulk and single particle study. The subject respirable particles of this work are smaller than the probing wavelength of light and much smaller than those that are likely to be considered in broad studies.⁴³

While the Mie–Bruggeman model shows great promise for analyzing mixed composition dust samples, it is new and not fully tested. Full testing awaits the production of size-specific microparticles of known and mixed composition on

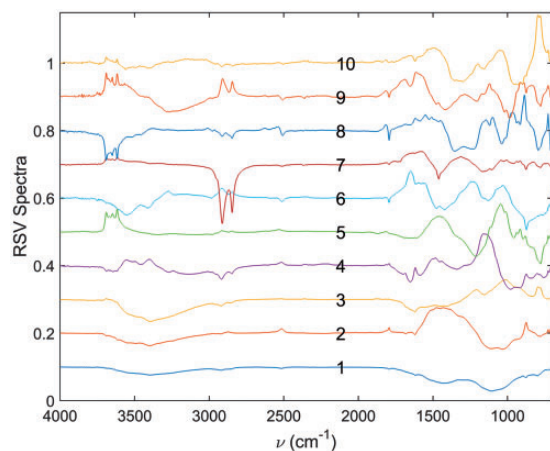


Figure 5. The top ten right singular vectors resulting from a singular value decomposition analysis of a matrix including the spectra of the three dust library samples, the calibrating particles, and some Mie–Bruggeman modeling results.

an individual particle basis (work continues on this). The following section describes a more conventional analysis using singular value decomposition, however this analysis is also enriched by the Mie–Bruggeman model.

Singular Value Decomposition Analysis

Each of the dust particle IR spectra were loaded as rows into a matrix \mathbf{X} with the dimensions of the number of particle spectra (m) by the number of spectral steps (n_s), which was 1651 for this work. The initial rows held the dust particle spectra (186 particles), later rows contained the IR spectra of calibrant particles (95 particles), and there was the option of adding more spectra from Mie–Bruggeman model predictions (110 particle simulations). Singular value decomposition (SVD) is applicable to rectangular matrices (like the \mathbf{X} matrix) and is closely related to eigen-analysis of square matrices. To make a square matrix out of the \mathbf{X} matrix, one can use the transpose (\mathbf{X}^T) in the form of $\mathbf{X} \cdot \mathbf{X}^T$ or $\mathbf{X}^T \cdot \mathbf{X}$, where the former is $m \times m$ and the latter is $n_s \times n_s$. SVD finds the eigenvectors of both $\mathbf{X} \cdot \mathbf{X}^T$ and $\mathbf{X}^T \cdot \mathbf{X}$ and connects them with a common set of eigenvalues, the square roots of which are known as the singular values and the number of these is the smaller of m or n_s . In this work (where $m < n_s$), the eigenvectors of $\mathbf{X}^T \cdot \mathbf{X}$ (right singular vectors or RSVs) look like IR spectra, while the eigenvectors of $\mathbf{X} \cdot \mathbf{X}^T$ (left singular vectors or LSVs) look like scores (one value for each right singular vector's dot product with each particle spectrum). SVD finds these solutions by decomposition rather than eigenvector routines, and in this sense is more mathematically powerful than principal component analysis (PCA), which can be thought of as a subset of SVD analysis.

Figure 5 shows the first 10 right singular vectors (RSVs) upon using an \mathbf{X} matrix with spectra of 186 dust particles,

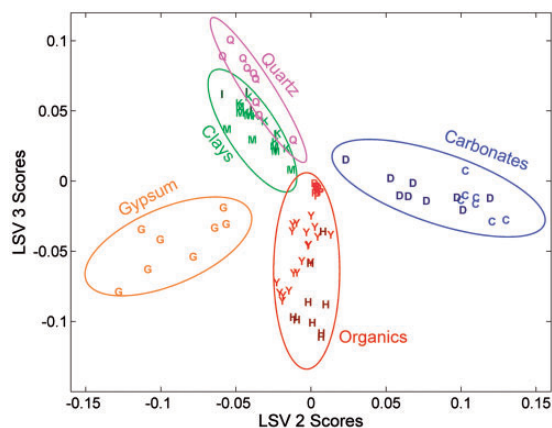


Figure 6. Left singular vectors or scores, LSV 3 versus LSV 2, for the calibrant particles. These scores amount to dot products of the chosen right singular vectors (shown in Figure 5) with the particle spectra of interest, in this case just the calibrants. The scores are plotted with letters indicating the calibrant: G for gypsum, M for montmorillonite clay, I for illite clay, K for kaolinite clay, Q for quartz, D for dolomite, C for calcite, P for polyethylene, Y for yeast, and H for humic acid/salt. The choice of LSV 3 versus LSV 2 shows good separation of the pure mineral calibrants. The ellipses were positioned and varied by hand to define the ranges of variation. Note how the major axes of the ellipses point outward.

95 calibrant particles, and 110 Mie–Bruggeman spectral simulations. The RSVs are analogous to the more commonly used principal components, i.e., they are ordered by their diminishing contributions to mathematical variations and are orthogonal to each other. They resemble IR spectra except that they have negative-going features owing to their orthogonal nature. The first (RSV 1) resembles the average spectrum and there are chemical clues in the features of these spectra. Organics, for instance by evidence of asymmetric (2920 cm^{-1}) and symmetric (2850 cm^{-1}) CH_2 stretches, are observable in all 10 RSVs, but prominent in RSV 7 and 9. The first 10 RSVs encompass $\sim 98\%$ of the change in the dust data set, however the data set is one of complex mixtures, so many of the higher numbered RSVs are not noisy and might be important for specific applications. The values in the left singular vectors are analogous to dot products of the dust particle spectra with the RSVs. A plot of LSV 3 versus LSV 2 scores for the dust particle calibrants is shown in Figure 6. Letters are used as symbols on the plot indicating the various calibrants. This plot shows that LSV 3 and LSV 2 scores are good at separating the pure mineral calibrants. There is some overlap between scores of silicates (quartz, clay calibrants such as kaolinite, illite, montmorillonite), but there are also well-separated groups of carbonates (dolomite, calcite), gypsum, and organics (yeast, humic acid/salt, polyethylene). These bigger groups are indicated with ellipses (for later comparison to the dust particles).

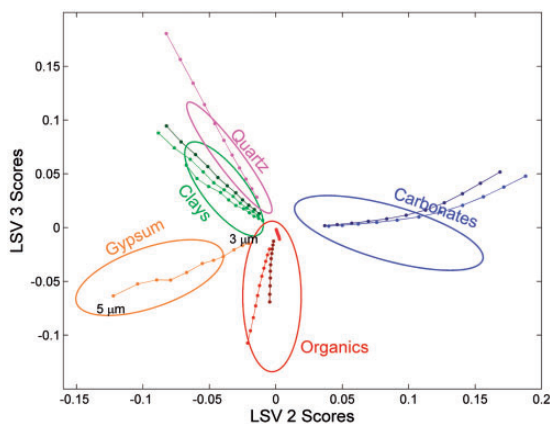


Figure 7. Left singular vectors or scores (LSV3 versus LSV 2) of Mie–Bruggeman models of pure calibrant particles as a function of particle size varying from 3 μm to 5 μm . The same ellipses from Figure 6 were redrawn here to indicate the range of variation of the calibrant data without cluttering the plot with the data points from Figure 6. The smallest particles have scores near the center, while increasing particle size trends towards the outside of the score space, so the biggest spread (the one along the major axes of the ellipses) is due to variation in particle size.

Before looking at the dust particle results, it is useful to examine the results of Mie–Bruggeman simulations of particle spectra of the pure calibrants as a function of particle size varying from 3 μm to 5 μm as shown in Figure 7. Again, LSV 3 scores are plotted against LSV 2 scores for direct comparison to experimental data in Figure 6. In terms of an LSV 3 versus LSV 2 plot, there is a systematic dependence of the scores on particle radii. Larger particle sizes push the scores to the outside of the plot. This suggests that small variations in particle size may be an important if not dominant source of spread on these plots. Taking gypsum as an example, it suggests that the experimental diameters range from ~ 4 μm to 5 μm . Similar analyses can be performed for other calibrants. The observation of size effect trends (indicated with lines in Figure 7) running along the major axis of ellipses characterizing spread, reveals that particle radius variation is the most important contributor to spreads in this analysis. Consequently, orientation and shape effects are the most likely contributors to the spreads perpendicular to the particle radius trends (lines in Figure 7), i.e., the minor axes of the ellipses. The combination of Mie–Bruggeman modeling with SVD scores presents the possibility of seeing beyond the dominant source of size spread that leaves the spreads of shape and orientation as the likely errors limiting the quantification of composition mixtures. It is also useful to predict the position of a uniform mixture of all the calibrants that will have scores near zero, the center of these plots. Noting that the organics are very different than minerals, we note that plots of LSV 9 versus LSV 3 are good at separating organics, but space constraints prevent showing plots of these results.

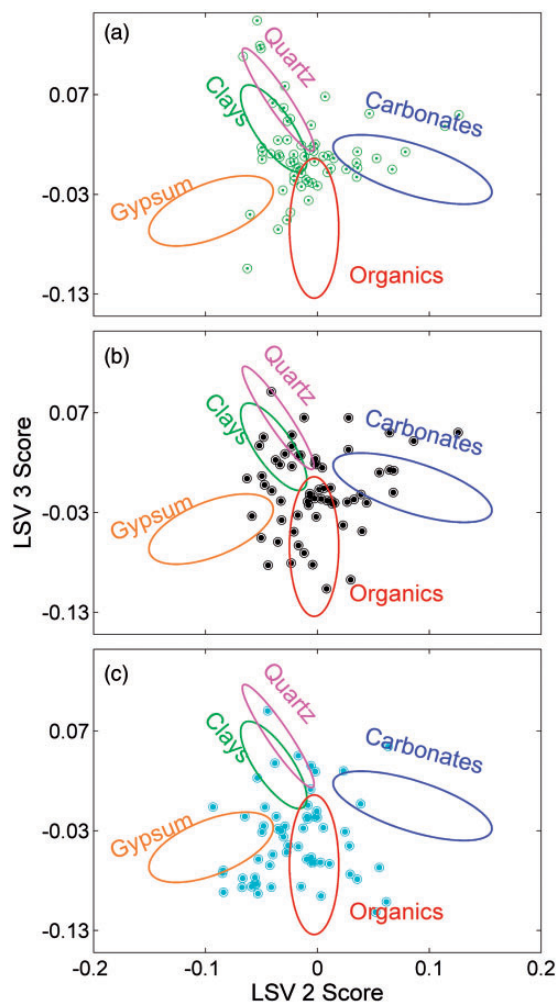


Figure 8. Left singular vectors or scores (LSV 3 versus LSV 2) for the three dust libraries: (a) lab air; (b) a house filter; (c) the 11 September 2001 WTC event. The ellipses show the range of variation of the calibrants whose particle data are given in Figure 6. Differences in the three samples are evident when compared to the calibrant materials.

With the above preparation, the scores of LSV 3 versus LSV 2 for the spectra of the three dust particle libraries are given in Figure 8. The calibrant data is not plotted, but the ellipses show the regions in which the calibrant data occurred. The data sets for lab air (Figure 8a), house filter (Figure 8b), and September 11, 2001 WTC (Figure 8c) do spread differently. Most of the scores do not fall within calibrant ellipses, hence the characterization of these dust particles as mixtures. On the other hand, the mixtures are not compressed into one distribution at the center that would correspond to uniform fractions of each calibrant. The lab air results (Figure 8a) show a major concentration between clay, quartz, and organics. The house filter scores (Figure 8b) show a concentration around organics suggesting that these particles are mostly all organic, or mixture of organics and other

components (clays, gypsum, quartz, and carbonates). Mie–Bruggeman modeling shows that mixtures of just two calibrant species will have scores that tend to lie on lines between the centers of the corresponding ellipses. For instance, the region between gypsum and organics is more populated as one goes from lab air to house filter to 11 September 2001 WTC. Similar results can be obtained to highlight organics present in the dust samples by plotting different pairwise combinations of LSVs (such as LSV 9 versus LSV 3) that separate polyethylene, yeast, and humic acid/salt into different groups. These results suggest that groupings of more than two LSV scores may reveal more information and are probably worth pursuing.

Conclusions

Scatter-free IR spectra of 186 individual particles from three different environments were recorded. When these results are combined with the 95 individual particle spectra of pure calibrant materials, they comprise a dust library, a resource for understanding dust particle samples. This dust library is different than other dust libraries as it was recorded from particles of a specific size ($\sim 4\ \mu\text{m}$) using plasmonic mesh that enhanced the absorption spectral features over those dominated by scattering. This helps to make analysis of complex mixtures easier. Note that these results can also predict extinction spectra, including extinction spectra for particles of other sizes or even distributions of sizes. The Mie–Bruggeman model for particles of mixed composition has been found useful for quantitative analysis in modeling the average spectrum of the dust particle library, although the absolute accuracy of volume fractions using the Mie–Bruggeman model is yet to be determined. Also note that the model can be improved by adding more calibrants as humic acid/salt has been added in this work. In view of this, the dust library was also analyzed by single value decomposition. Right singular vectors for the current dust library have been presented (which are like more commonly used spectral principal components). Left singular vectors were used like principal component scores to give insights on the chemical identity of the different dust particle samples. The lab air dust was found to have organics, clays, and quartz as major components, the house filter dust was dominated by organics, and the respirable WTC dust was dominated by the dry wall component, gypsum. The Mie–Bruggeman model was also found to enrich the interpretation of the SVD results. The tools developed herein will help to analyze the chemical composition of dust samples including particles of the largest sizes that get into human lungs. The information will help to inform health studies associated with particulate matter of the smallest of “coarse” particle distributions that are slightly larger and somewhat overlapped with the “fine” particle distributions that are currently well regulated.

Acknowledgements

We thank the Robert H. Edgerley Environmental Toxicology Fellowship Fund for support of AL, the Ohio State University Office of Energy and Environment Sustainability Research Project for support of SL, and Dr. Paul J. Lioy, Professor and Vice Chair at Department of Environmental Medicine, UMDNJ – Robert Wood Johnson Medical School, NJ for providing us with the WTC dust sample.

Declaration of Conflicting Interests

The authors report there are no conflicts of interest.

Funding

This work was supported by the National Science Foundation (grant number CHE 1213293).

Supplemental Material

All supplemental material mentioned in the text, including details of the Mie fit for humic acid/salt, is available at <http://asp.sagepub.com/supplemental>.

References

1. F. Dominici, A. McDermott, S.L. Zeger, J.M. Samet. “National Maps of the Effects of Particulate Matter on Mortality: Exploring Geographical Variation”. *Environ. Health Persp.* 2003. 111(1): 39–43.
2. M.L. Bell, K. Ebisu, R.D. Peng, J.M. Samet, F. Dominici. “Hospital Admissions and Chemical Composition of Fine Particle Air Pollution”. *Am. J. Respir. Crit. Care Med.* 2009. 179(12): 1115–1120.
3. P. Eastwood. *Particulate Emissions from Vehicles*. Chichester, England, Hoboken, NJ: John Wiley and Sons, 2008.
4. L. Morawska, T. Salthammer. “Indoor Environment: Airborne Particles and Settled Dust”. In: L. Morawska, T. Salthammer (eds). *Weinheim, Germany: Wiley-VCH Verlag GmbH & Co. KGaA*, 2006.
5. U.S. Environmental Protection Agency. “Air Quality Criteria for Particulate Matter (Final Report, April 1996)”. Washington, DC, 1996. Fig. 13.13.
6. W. Hofmann. “Modelling Inhaled Particle Deposition in the Human Lung—A Review”. *J. Aerosol Sci.* 2011. 42(10): 693–724.
7. W.C. Hinds. “Aerosol Technology: Properties, Behavior, and Measurement of Airborne Particles”. New York, NY: J. Wiley, 1982.
8. F.R. Spellman and N.E. Whiting. *Environmental Engineer’s Mathematics Handbook*. New York: CRC Press, 2004.
9. R.D. Peng, H.H. Chang, M.L. Bell, A. McDermott, S.L. Zeger, J.M. Samet, F. Dominici. “Coarse Particulate Matter Air Pollution and Hospital Admissions for Cardiovascular and Respiratory Diseases Among Medicare Patients”. *JAMA.* 2008. 299(18): 2172–2179.
10. D.B. Lioy, K.E. Cilwa, M. McCormack, M.A. Malone, J.V. Coe. “Infrared Spectral Model for Subwavelength Particles of Mixed Composition Based on the Spectra of Individual Particles with Calibration Data for Airborne Dust”. *J. Phys. Chem. A.* 2013. 117(44): 11297–11307.
11. M.A. Malone, S. Prakash, J.M. Heer, L.D. Corwin, K.E. Cilwa, J.V. Coe. “Modifying Infrared Scattering Effects of Single Yeast Cells with Plasmonic Metal Mesh”. *J. Chem. Phys.* 2010. 133(18): 7.
12. K.E. Cilwa, M. McCormack, M. Lew, C. Robitaille, L. Corwin, M.A. Malone, J.V. Coe. “Scatter-Free IR Absorption Spectra of Individual, 3–5 μm , Airborne Dust Particles Using Plasmonic Metal Microarrays: A Library of 63 Spectra”. *J. Phys. Chem. C.* 2011. 115(34): 16910–16919.
13. M.A. Malone, K.E. Cilwa, A. Luthra, M. McCormack, D. Lioy, J.V. Coe. “Plasmonics under the Infrared Microscope: Sensing and Spectra of

- Single Particles Using Metal Film Hole Arrays". *Photonics and Optoelectronics (SOPO), 2012 Symposium*. 2012. 1(6): 21–23.
14. A. Ravi, M.A. Malone, A. Luthra, D. Lioi, J.V. Coe. "Spectral Challenges of Individual Wavelength-Scale Particles: Strong Phonons and their Distorted Lineshapes". *PCCP*. 2013. 15(25): 10307–10315.
 15. J.V. Coe, D.B. Lioi, L. Shaffer, M.A. Malone, A. Luthra, A. Ravi. "Plasmonic Spectra of Individual Subwavelength Particles under the Infrared Microscope: Cells and Airborne Dust". *Proc. SPIE* 2014. 8957 (Plasmonics in Biology and Medicine XI): 89570A/89571–89570A/89579.
 16. A. Reff, B.J. Turpin, J.H. Offenberg, C.P. Weisel, J. Zhang, M. Morandi, T. Stock, S. Colome, A. Winer. "A Functional Group Characterization of Organic PM_{2.5} Exposure: Results from the RIOPA Study". *Atmos. Environ.* 2007. 41(22): 4585–4598.
 17. A. Fahey, K.D. McKeegan, S.A. Sandford, R.M. Walker, B. Wopenka, E. Zinner. "Complementary Laboratory Measurements of Individual Interplanetary Dust Particles". *Astrophys. Space Sci. Libr.* 1985. 119(Prop. Interact. Interplanet. Dust): 149–155.
 18. B. Wopenka, P.D. Swan. "Micro-FTIR Measurements on Individual Interplanetary Dust Particles". *Mikrochim. Acta.* 1988. 1(1–6): 183–187.
 19. M. Abdul Malek, B.W. Kim, H.-J. Jung, Y.-C. Song, C.-U. Ro. "Single-Particle Mineralogy of Chinese Soil Particles by the Combined Use of Low-Z Particle Electron Probe X-ray Microanalysis and Attenuated Total Reflectance-FT-IR Imaging Techniques". *Anal. Chem.* 2011. 83(20): 7970–7977.
 20. Y.C. Song, H.J. Eom, H.J. Jung, M.A. Malek, H.K. Kim, H. Geng, C.U. Ro. "Investigation of Aged Asian Dust Particles by the Combined Use of Quantitative ED-EPMA and ATR-FTIR Imaging". *Atmos. Chem. Phys.* 2013. 13(6): 3463–3480.
 21. G.J. Flynn, L.P. Keller, C. Jacobsen, S. Wirick. "Elemental Mapping and X-ray Absorption Near-Edge Structure (XANES) Spectroscopy with a Scanning Transmission X-ray Microscope". *Meteorit. Planet. Sci.* 1999. 34: A36–A36.
 22. S.A.E. Johansson. "Particle Induced X-ray Emission and Complementary Nuclear Methods for Trace Element Determination. Plenary lecture". *Analyst.* 1992. 117(3): 259–265.
 23. S.H. Lee, D.M. Murphy, D.S. Thomson, A.M. Middlebrook. "Chemical Components of Single Particles Measured with Particle Analysis by Laser Mass Spectrometry (PALMS) During the Atlanta SuperSite Project: Focus on Organic/Sulfate, Lead, Soot, and Mineral Particles". *J. Geophys. Res.-Atmos.* 2002. 107D1–D2).
 24. D.M. Murphy, D.S. Thomson. "Laser Ionization Mass-Spectroscopy of Single Aerosol-Particles". *Aerosol Sci. Technol.* 1995. 22(3): 237–249.
 25. A. Turner, L. Simmonds. "Elemental Concentrations and Metal Bioaccessibility in UK Household Dust". *Sci. Total Environ.* 2006. 371(1–3): 74–81.
 26. T. Dunder, R.E. Miller. "Infrared-Spectroscopy and Mie Scattering of Acetylene Aerosols Formed in a Low-Temperature Diffusion Cell". *J. Chem. Phys.* 1990. 93(5): 3693–3703.
 27. C. Christiansen. "Untersuchungen über die optischen Eigenschaften von fein vertheilten Körpern". *Annalen der Physik.* 1884. 298–306.
 28. D. Brownlee, P. Tsou, J. Aleon, et al. "Research Article – Comet 81P/Wild 2 Under a Microscope". *Science.* 2006. 314(5806): 1711–1716.
 29. P. Dumas, G.L. Carr, G.P. Williams. "Enhancing the Lateral Resolution in Infrared Microspectrometry by Using Synchrotron Radiation: Applications and Perspectives". *Analisis.* 2000. 28(1): 68–74.
 30. P.I. Raynal, E. Quirico, J. Borg, D. Deboffe, P. Dumas, L. d'Hendecourt, J.P. Bibring, Y. Langevin. "Synchrotron Infrared Microscopy of Micron-Sized Extraterrestrial Grains". *Planet. Space Sci.* 2000. 48(12–14): 1329–1339.
 31. M.A. Malone, K.E. Cilwa, M. McCormack, J.V. Coe. "Modifying an Infrared Microscope to Characterize Propagating Surface Plasmon Polariton-Mediated Resonances". *J. Phys. Chem. C.* 2011. 115(25): 12250–12254.
 32. J. Heer, L. Corwin, K. Cilwa, M.A. Malone, J.V. Coe. "Infrared Sensitivity of Plasmonic Metal Films with Hole Arrays to Microspheres In and Out of the Holes". *J. Phys. Chem. C.* 2010. 114: 520–525.
 33. K.E. Cilwa, K.R. Rodriguez, J.M. Heer, M.A. Malone, L.D. Corwin, J.V. Coe. "Propagation Lengths of Surface Plasmon Polaritons on Metal Films with Arrays of Subwavelength Holes by Infrared Imaging Spectroscopy". *J. Chem. Phys.* 2009. 131(1): 061101–061105.
 34. M.A. Malone, M. McCormack, J.V. Coe. "Single Airborne Dust Particles using Plasmonic Metal Films with Hole Arrays". *J. Phys. Chem. Lett.* 2012. 3(6): 720–724.
 35. U.S. Environmental Protection Agency. "Report to Congress on Indoor Air Quality. Volume 2: Assessment and Control of Indoor Air Pollution". Washington, DC: U.S. Environmental Protection Agency, 1989.
 36. P.J. Lioy, C.P. Weisel, J.R. Millette, et al. "Characterization of the Dust/Smoke Aerosol that Settled East of the World Trade Center (WTC) in Lower Manhattan after the Collapse of the WTC 11 September 2001". *Environ. Health Perspect.* 2002. 110(7): 703–714.
 37. P.J. Lioy. *DUST: The Inside Story of its Role in the September 11th Aftermath*. Landham MD: Rowman & Littlefield Publishing Group, 2011.
 38. H.C. van de Hulst. *Light Scattering by Small Particles*. New York: Dover, 1981.
 39. M.I. Mishchenko, A.A. Lacis, B.E. Carlson, L.D. Travis. "Nonsphericity of Dust-like Tropospheric Aerosols – Implications for Aerosol Remote-Sensing and Climate Modelling". *Geophys. Res. Lett.* 1995. 22(9): 1077–1080.
 40. C.F. Bohren, D.R. Huffman. *Absorption and Scattering of Light by Small Particles*. New York: John Wiley & Sons, 1983.
 41. P.W. Bevington. *Data Reduction and Error Analysis for the Physical Sciences*. New York: McGraw-Hill, 1969.
 42. J.K. McGee, L.C. Chen, M.D. Cohen, et al. "Chemical Analysis of World Trade Center Fine Particulate Matter for use in Toxicologic Assessment". *Environ. Health Perspect.* 2003. 111(7): 972–980.
 43. P.J. Lioy, C.P. Weisel, J.R. Millette, et al. "Characterization of the Dust/Smoke Aerosol that Settled East of the World Trade Center (WTC) in Lower Manhattan after the Collapse of the WTC 11 September 2001". *Environ. Health Perspect.* 2002. 110(7): 703–714.